

High-speed and drop-on-demand printing with a pulsed electrohydrodynamic jet

This article has been downloaded from IOPscience. Please scroll down to see the full text article.

2010 J. Micromech. Microeng. 20 095026

(<http://iopscience.iop.org/0960-1317/20/9/095026>)

View [the table of contents for this issue](#), or go to the [journal homepage](#) for more

Download details:

IP Address: 75.237.155.60

The article was downloaded on 22/08/2010 at 00:18

Please note that [terms and conditions apply](#).

High-speed and drop-on-demand printing with a pulsed electrohydrodynamic jet

S Mishra, K L Barton, A G Alleyne, P M Ferreira and J A Rogers

University of Illinois, Urbana, IL 61801, USA

E-mail: sandipan@illinois.edu

Received 5 April 2010, in final form 4 June 2010

Published 20 August 2010

Online at stacks.iop.org/JMM/20/095026

Abstract

We present a pulsed dc voltage printing regime for high-speed, high-resolution and high-precision electrohydrodynamic jet (E-jet) printing. The voltage pulse peak induces a very fast E-jetting mode from the nozzle for a short duration, while a baseline dc voltage is picked to ensure that the meniscus is always deformed to nearly a conical shape but not in a jetting mode. The duration of the pulse determines the volume of the droplet and therefore the feature size on the substrate. The droplet deposition rate is controlled by the time interval between two successive pulses. Through a suitable choice of the pulse width and frequency, a jet-printing regime with a specified droplet size and droplet spacing can be created. Further, by properly coordinating the pulsing with positioning commands, high spatial resolution can also be achieved. We demonstrate high-speed printing capabilities at 1 kHz with drop-on-demand and registration capabilities with 3–5 μm droplet size for an aqueous ink and 1–2 μm for a photocurable polymer ink.

(Some figures in this article are in colour only in the electronic version)

1. Introduction

Jet printing-based manufacturing processes at the nano- and micro-scales have been the target of much research because of the ability to generate very small-scale droplets. Examples of jet printing include the now ubiquitous ink-jet printing using thermal and piezo-excitation, and E-jet printing. Among these, E-jet printing has demonstrated superior resolution, printing of micron and sub-micron scale droplets using a wide variety of inks [1–4]. However, the speed of the process and its ability to produce uniform printing quality have been cited as impediments, as pointed out in a review on E-jet [5].

Because of the ability to print high-resolution droplets and lines with a range of inks, E-jet printing has shown tremendous promise for applications such as printing metallic (Ag) interconnects for printed electronics [2], bio-sensors [1, 4], etc. As the advantages of E-jet printing become more apparent (e.g. the potential for purely additive operations, the ability to directly print biological materials, maskless lithography), additional features like drop-on-demand functionality and the ability to precisely control droplet sizes become necessary. Further, enhanced process controls to independently regulate process outputs such as droplet size and delivery frequency

become critical. Finally, as with any manufacturing process, throughput rates (in this case, printing speeds) and process robustness are key decision parameters in the adoption of the process. Therefore, to fully realize the capability of the E-jet printing process, this research reports on how to exploit input voltage modulation to enhance droplet deposition rates, obtain consistent droplet volume and accurate spatial placement of droplets.

E-jet printing uses electric-field induced fluid flows through fine micro capillary nozzles to create devices in the micro- and nano-scale range [1]. Typically, these electric fields are created by establishing a constant voltage difference between the nozzle carrying the ink (the print head) and the print substrate. The electric field attracts ions in the fluid toward the substrate, deforming the meniscus to a conical shape and eventually leading to instability that results in droplet release from the apex of the cone [1, 6]. Electrohydrodynamic discharge from a nozzle results naturally in a pulsed flow. This was exploited by Chen [9] to accurately place drops. Juraschek and Rollgen [7] reported that this pulsing persists in the spray regime reporting both low-frequency 10 Hz and high-frequency 1 kHz pulsations in an electrohydrodynamic spray. To exploit this natural pulsation,

Chen *et al* [9] and Choi *et al* [8] have developed scaling laws for characterizing E-jet. Until now, high-resolution E-jet printing has used this natural pulsation and is therefore limited by the natural pulsating frequency of the aforementioned discharge, which has substantial variability. To overcome this limitation, Kim *et al* [10] suggested the use of a piezoelectric excitation of the nozzle tip (hybrid jet printing) along with electric field induced jetting. Pulsing of ac has been demonstrated for E-jet by Nyugen *et al* [11]. Modulation of ac showed advantages over dc voltage in terms of fabrication of nozzles, droplet repulsion and drop-on-demand capabilities based on the frequency of sinusoidal voltage applied. Kim *et al* [12] used a square wave dc for E-jet printing and used the amplitude of the voltage to control the droplet size. Stachewicz *et al* [13] demonstrated a single-event pulsed droplet generation for E-jet, as well as a study of relaxation times for drop-on-demand electro spraying [14].

In the literature cited above, the droplet diameters and pulse frequencies have been limited to size $50\ \mu\text{m}$ and printing frequencies of 25 Hz. Further, to the best of our knowledge, no systematically controlled high-speed printing regimes have been developed for delivering precise droplet volumes with high fidelity spatial and temporal resolution. This paper presents a manufacturing oriented approach to pulsed input voltage E-jet printing including (1) high-speed printing, (2) high-resolution printing and (3) a well-documented recipe for shaping the pulse signal.

In this paper, we present an E-jet printing mode capable of high speeds and independent control of the droplet size and printing frequency. Specifically, this mode demonstrates capability for printing speeds of 1000 droplets per second, while producing consistent and controllable droplet sizes of $3\text{--}6\ \mu\text{m}$. This mode uses a pulsed voltage signal to generate electrohydrodynamic flow from the nozzle. The pulse peak is chosen so as to induce a very fast E-jetting mode from the nozzle, while the baseline voltage is picked to ensure that a near conical shaped meniscus is always present, but not discharging any fluid. The duration of the pulse determines the volume of the droplet and therefore the feature size on the substrate. On the other hand, the droplet deposition rate is controlled by varying the time interval between two successive pulses. Through suitable choice of the pulse width and frequency, a jet-printing regime with specified feature size and deposition rate can be created.

The rest of the paper is organized as follows. Section 2 provides an introduction to the E-jet printing process. Section 3 then discusses a novel voltage modulation scheme for delivering high-speed high-resolution E-jet printing capabilities. A design recipe for determining the parameters for this scheme is described in section 4. Sections 5 describes the experimental E-jet printing testbed. Sections 6 and 7 demonstrate high-speed printing and drop-on-demand printing capabilities of the voltage modulated printing regime. Finally, in section 8 the contribution of this paper is summarized.

2. Electrohydrodynamic jet printing

Figure 1 presents a schematic of the E-jet printing process. As can be seen from figure 1, the main elements for E-jet

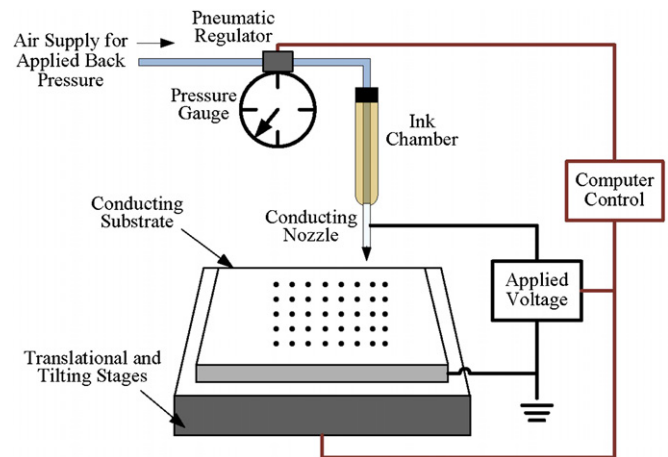


Figure 1. Schematic of the E-jet printing set-up including nozzle and ink chamber, air supply for back pressure, conducting substrate, and translation and tilting stages.

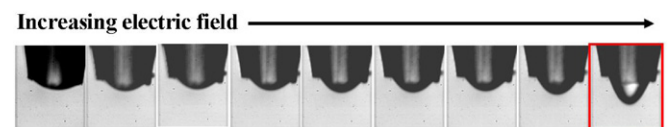


Figure 2. Illustration of the change in the meniscus of the fluid due to an increase in voltage potential between the nozzle tip and the substrate.

printing include an ink chamber, metal-coated glass nozzle tip, substrate and positioning system. The controllable printing process parameters are the back pressure (pneumatic) applied to the ink chamber, the offset height between the nozzle and substrate and the applied voltage potential between a conducting nozzle tip and substrate. Note that the nozzle tip and substrate are generally coated with metal to ensure conductivity.

A voltage applied to the nozzle tip causes mobile ions in the ink to accumulate near the surface at the tip of the nozzle. The mutual Coulomb repulsion between the ions introduces a tangential stress on the liquid surface, thereby deforming the meniscus into a conical shape [1]. At some point, the electrostatic stress overcomes the surface tension of the meniscus and droplets eject from the cone. Figure 2 illustrates the change in the ink meniscus due to an increase in voltage. Depending on the fluid properties, as the applied field is increased this discharge begins as a pulsed or intermittent jet (pre-jet modes) transitioning into a stable single jet, multiple unstable jets and finally becoming a spray for very large electric field strengths. Each of the different jetting modes (e.g. pulsating, stable jet, E-spray [15]) can be used to achieve various printing/spraying applications. Pre-jet modes are typically used for printing because of better controllability at high speeds.

Changes in back pressure, stand-off height and applied voltage affect the size and frequency of the droplets. This sensitivity of the process output to variations under the printing conditions requires high-resolution sensing and control in order to achieve stable and predictable printing results.

3. Voltage modulation in E-jet printing

Typically, the jet frequency and droplet diameter have been controlled by changing the applied voltage difference across the tip and the substrate. From a process development point of view, this has significant disadvantages. First, for a given nozzle diameter, printing ink and stand-off height (distance of the nozzle tip from the substrate), the droplet diameter on the surface (D) and jetting frequency (f) are coupled. Scaling laws from Choi *et al* [8] capture this dependence with the following equations:

$$f = \frac{E^{\frac{3}{2}}}{d_N} \quad \text{and} \quad d = \frac{\sqrt{E}}{d_N} \quad (1)$$

$$D = dF(\theta), \quad (2)$$

where d_N is the anchoring radius of the meniscus, d is the droplet diameter of the ejected droplet, E is the electric field because of the applied potential and θ is the contact angle at the surface; $F(\theta)$ is a function of the contact angle θ . As can be seen from the above equations, one can set a voltage level to either obtain a desired droplet diameter or a printing speed (droplets/sec), but not both. The second disadvantage associated with printing by setting a constant voltage different between the tip and substrate accrues from the fact that minute changes in the stand-off height (for example, because of small misalignments or errors associated with the motion stage) can cause significant changes in the jetting frequency and droplet diameters.

With a sufficiently high potential difference, very fast jetting frequencies of several kHz can be achieved. However, at the resulting strong electric field, the system becomes more sensitive to variations under operating conditions such as stand-off height, meniscus wetting properties, etc and the jetting frequency may vary substantially during printing, leading to inconsistent droplet spacing. Therefore, constant high-voltage E-jetting is unsuitable for printing large droplet arrays with regular droplet diameters and consistent droplet spacing (as might be required in a DNA microarray, for example). At the same time, low-voltage E-jetting results in slow printing speeds (with droplet deposition rates of 1–5 drops per second).

In order to be able to overcome these limitations, we propose a short-time high-voltage pulse superimposed over a lower baseline constant voltage. The short high-voltage pulse releases a droplet (or a finite number of droplets) from the nozzle, while the lower constant voltage holds the charge in the meniscus. Figure 3 shows the time plot of a typical pulse. The duration of the pulse controls the number of droplets released. These droplets coalesce and form a larger droplet on the substrate surface. Hence the volume of fluid deposited on the substrate is controlled by the number of droplets released per high-voltage pulse and consequently, the duration of this pulse. On the other hand, the time between two pulses determines the time or (for constant velocity motion of the stage) distance (s) between successive droplets on the substrate.

The baseline voltage must be chosen such that there is no jetting at that voltage; however, it must be large enough

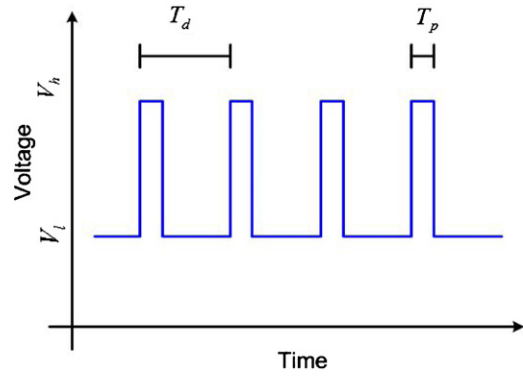


Figure 3. Schematic time plot of the voltage profile for the pulsed E-jet. T_d denotes the time between successive pulses while T_p denotes the pulse width. V_h and V_l are the high and low voltages respectively.

to ensure that the Taylor cone [16] is formed and maintained at the tip of the micro capillary nozzle. On the other hand, the pulse peak voltage V_h is chosen such that it results in a very fast natural jetting mode with a frequency of jetting given by f_h . By adjusting the pulse peak voltage to a large enough value, it is possible to get f_h of the order of 10–50 kHz for most inks [1, 9].

3.1. Pulse spacing T_d

The pulse spacing T_d directly controls the droplet spacing on the substrate. This is because the distance between droplets can be changed by adjusting the time between successive pulses and the speed of movement (w_{st}) of the substrate with respect to the nozzle tip. The droplet spacing is given by $s_d = w_{st}T_d$.

3.2. Pulse width T_p

Assuming a hemispherical droplet of D on the surface of the substrate, we have (for $f_h T_p > 2$)

$$f_h v_h T_p = \frac{\pi}{12} D^3, \quad (3)$$

where v_h is the volume of a single droplet released from the nozzle and T_p is the pulse width. Given a fixed V_h (pulse peak), f_h and v_h are fixed. Therefore we can control the diameter of the deposited droplets by changing the pulse width T_p . Further, the size of these ‘aggregated’ droplets is more uniform than each individual discharged droplet because of the averaging effect. For a small enough pulse width, there may be no droplet released from the tip because of the time delay in formation of the meniscus and ejection of the droplet. This minimum possible T_p is dependent on the choice of V_h (see figure 13 for an example of a recorded input voltage pulse and the resulting current signal). Figure 4 shows a plot of this relationship for a photocurable polyurethane polymer (Norland Optical Adhesive NOA 73).

Therefore, by adjusting T_p and T_d we can fix the desired droplet diameter and spacing *independently*.

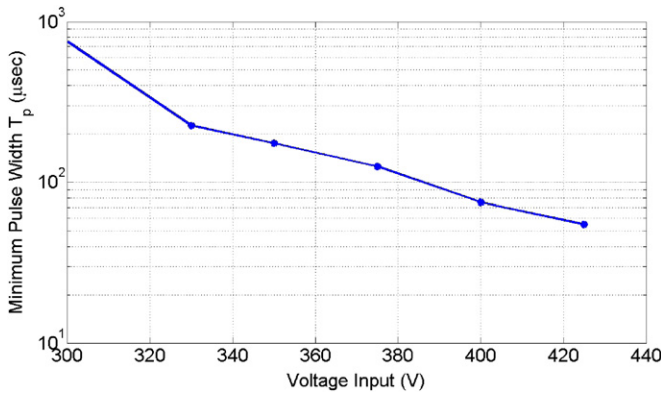


Figure 4. Plot of the minimum pulse width T_p against the input voltage V_h for a polyurethane polymer ink. For larger voltages, we can obtain droplet ejection for smaller pulse widths. For $V_h = 425$ V, we obtain $f_h > 18$ kHz.

4. Design recipe

In this section, we algorithmically describe how the input parameters, specifically the pulse modulation parameters V_h , V_l , T_p and T_d are determined, based on output requirements of the printing process, such as droplet spacing and droplet (feature) size.

- (i) Set process parameters: ink type, substrate type, back pressure (psi), and nozzle diameter. Typically, the nozzle diameter is chosen to be between 2 and 5 times the desired droplet diameter, while the back pressure is chosen so that it holds a spherical meniscus at the nozzle tip.
- (ii) Set V_l to be 5–10 V less than the initial voltage required to release a single droplet. (This voltage to release a droplet can be arrived at by gradually raising the voltage until the first drop is released from the nozzle.)
- (iii) Determine the substrate velocity (fastest possible, subject to motion stage hardware constraints) w_{st} .
- (iv) Determine the time between pulses as $T_d = \frac{s_d}{w_{st}}$, where s_d is the desired spacing between droplets.
- (v) Evaluate the potential V_h range so that
 - (a) V_h is significantly less than spraying, unstable jetting or arcing voltage.
 - (b) V_h is greater than the voltage that results in a jetting frequency of $f_{h,\min}$ which satisfies $f_{h,\min} T_d > 2$.
- (vi) Choose V_h to be as large as possible without violating (a) above. Determine the pulse width T_p to ensure the desired droplet diameter D , based on equation (2).

5. System description

To validate the feasibility of both the high-speed and drop-on-demand E-jet printing process, the design scheme described in the previous section was implemented on an experimental E-jet printing testbed shown in figure 5. Table 1 describes the hardware components of the system.

As can be seen from figure 5, the motion control system consists of five physically connected axes (X , Y , Z , U , A), a substrate mount, a nozzle mount and a camera for nozzle

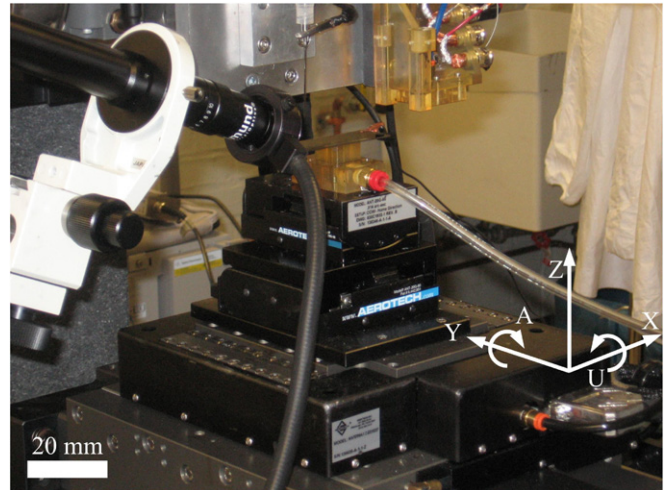


Figure 5. 5-axis experimental testbed for E-jet printing.

Table 1. System components.

Part	Manufacturer	Resolution
X , Y , Z stages	Aerotech	0.01 μm
Infinity 3 camera	Lumenera	2 Mpixel
Zoom lens	EdmundOptics NT55-834	2.5 \times –10 \times
Illuminator	EdmundOptics NT55-718	N/A
Voltage amplifier	Trek 677B	1V
Current detector	Femto NT59-178	1 nA

alignment and jetting visualization. The translational motion of the substrate is controlled through the X , Y axes, while the pitch and yaw are fixed through the U , A axes. The electrical connection to the nozzle and substrate, along with the substrate-side measurement scheme, followed the set-up illustrated in figure 10. The measured current signal was detected online and processed off-line to determine jetting information. The printing was done on a glass slide substrate coated with Au for conductivity. No other post-processing of the substrate was done. The standoff height for printing was set at 30 μm along the Z axis. For the interested reader, the effect of the stand-off height has been investigated in [8]. The power supply used is bipolar; however, for this paper, we will use positive polarity of the nozzle for demonstrating printing.

We now present printing results for (a) high-speed printing, and (b) drop-on-demand printing in the following sections.

6. High-speed printing results

The pulsed E-jet printing can significantly enhance printing speeds (droplet deposition rate). Typically in constant jet mode printing applications, jetting frequencies are around 1–5 droplets per second [1]. A graphics art rendered pattern 1.5 mm by 0.3 mm was used as a basis for comparison of printing speeds for constant voltage and pulsed voltage E-jet printing. The constant voltage printing was executed at 1 droplet per second jetting frequency and required ≈ 2200 s for printing. On the other hand, using pulsed jetting at 60 droplets per second the pattern was printed in 70 s.

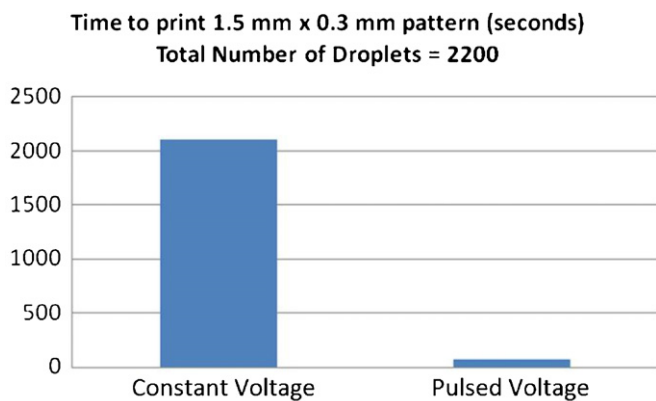


Figure 6. Chart showing printing times for 1.5 mm by 0.3 mm pattern using a constant voltage jet-printing mode and pulsed voltage printing jet mode. Pulsed voltage printing required 70 s, while constant voltage jet printing required 2200 s.

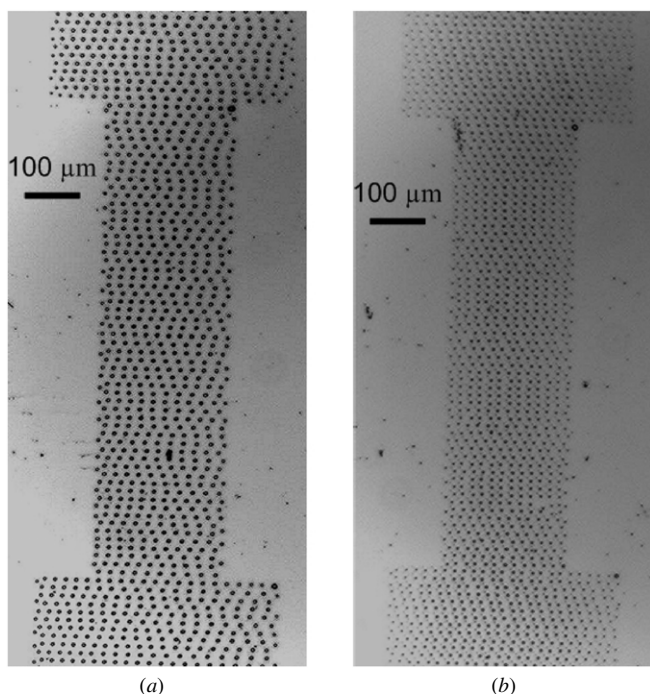


Figure 7. (a) Printed pattern using constant voltage jetting (5 μm capillary, phosphate buffer solution with 10% glycerol (vol.)). Total area = 0.3 mm × 1.5 mm. (b) Printed pattern using pulsed voltage jetting (5 μm capillary, phosphate buffer solution with 10% glycerol (vol.)) 0.3 mm × 1.5 mm. Printing with constant jetting resulted in irregular droplet spacing and size and required 2200 s. Printing with pulsed jetting resulted in regular droplet spacing, consistent droplet sizes and was completed in 70 s. Typical droplet diameter was 3 μm.

Figure 7 shows optical micrographs of the printed patterns obtained from the two printing methods. As shown in the chart in figure 6, the printing time was cut down by a factor of 30 using the pulsed mode operation. The droplet placement accuracy using the pulsed mode operation is critically dependent on the synchronization of the stage movement and the voltage pulsing. This is the source of the irregular droplet alignment from one raster to the next in figure 7.

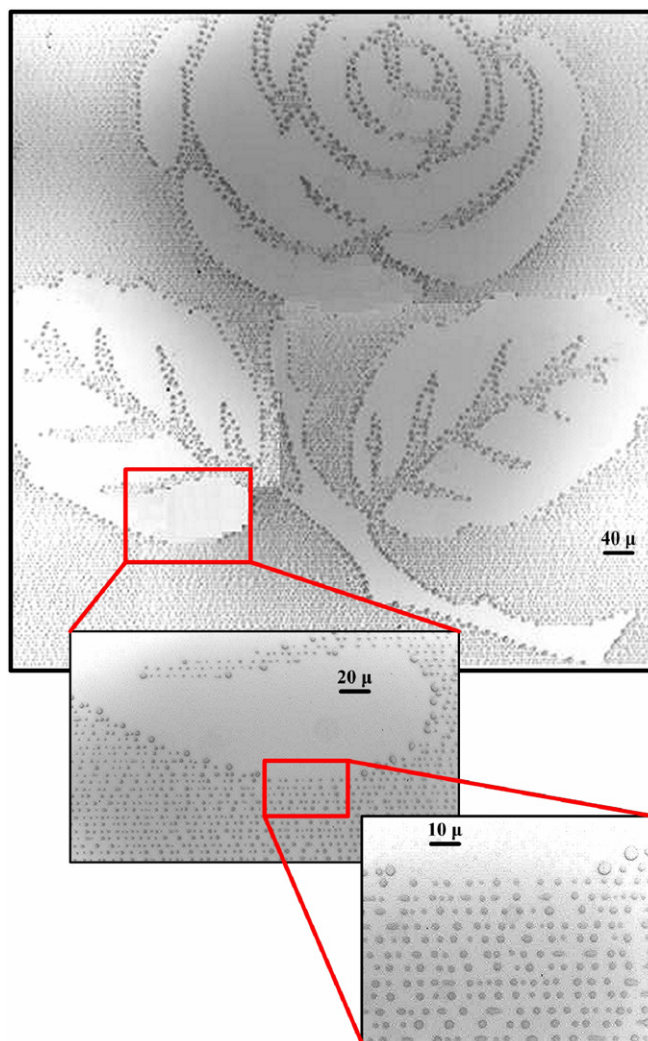


Figure 8. Printed pattern using NOA 73 (photocurable polyurethane polymer) at 1 kHz printing frequency using a 2 μm ID capillary nozzle. The droplet diameter varied from 1 to 2 μm.

Further, pulsed E-jetting shows tremendous potential for establishing printing speeds well into several kHz that will transform this technology into a viable nano-manufacturing process. Figure 8 illustrates an image printed at 1 kHz with droplet sizes ranging from 1 to 2 μm. Printed lines can be laid down on a substrate at speeds up to 10 kHz, shown in figure 9.

7. Drop-on-demand printing

7.1. Current detection

Monitoring the E-jet process optically becomes very challenging especially with printing at single micron resolutions and speeds approaching 1000 droplets per second. Therefore, a scheme based on current monitoring is developed for the process. Essentially, the E-jet process involves combined mass and charge transfer between the nozzle and substrate, i.e. each droplet released from the nozzle carries a net positive or negative charge [3], depending on the direction

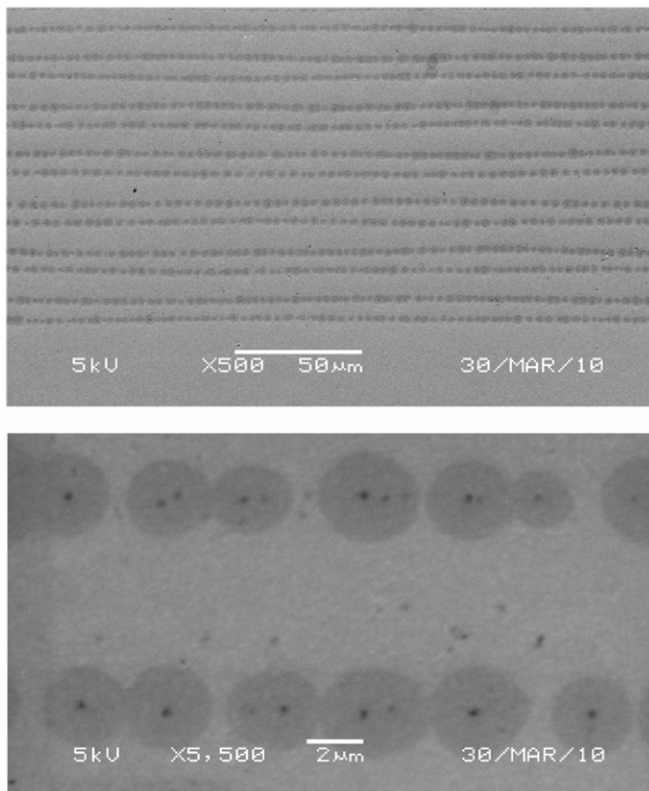


Figure 9. SEM images of printed lines using NOA 73 (photocurable polyurethane polymer) at 10 kHz printing frequency using a 2 μm ID capillary nozzle. The zoomed-in detail on the right shows the spreading of the droplets after printing.

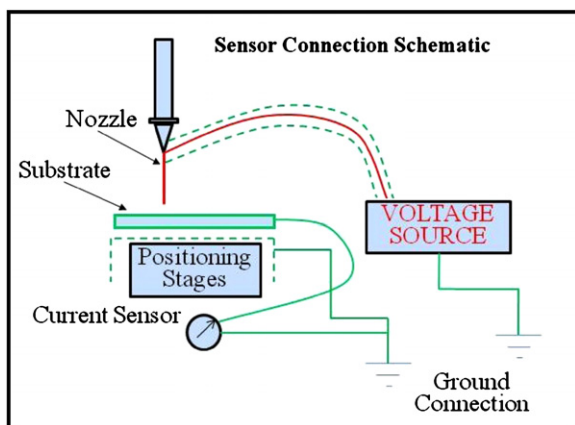


Figure 10. Schematic of the substrate-side current measurement set-up for the E-jet process.

of the applied field. With the release of each charged droplet from the nozzle, a small current is drawn to neutralize the resulting charge imbalance in the fluid at the meniscus. By detecting this current, the time of droplet release can be determined. This measurement scheme is termed nozzle-side measurement. An alternate scheme measures the current dissipated through the substrate to ground when a charged droplet from the nozzle arrives at a conductive substrate. This current can be measured by introducing a current sensor in

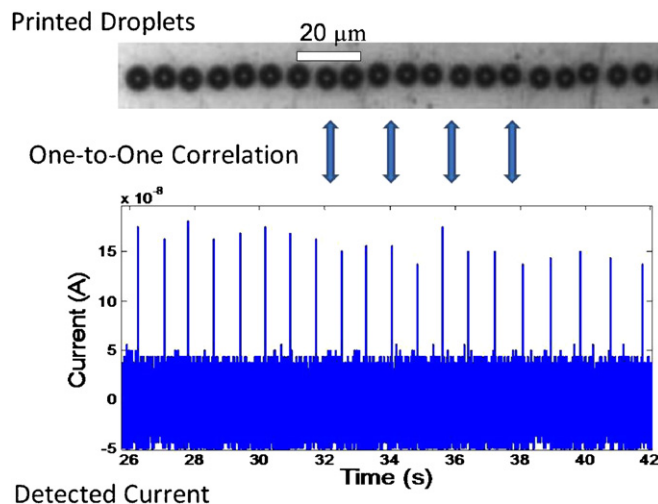


Figure 11. Illustration of the one-to-one correlation between the printed droplets and the measured current peaks.

the substrate-ground connection. This measurement scheme is termed substrate-side measurement. Figure 10 shows a schematic of substrate-side current measurement set-up. The high-voltage source is connected to the nozzle side, while a current sensor is connected to the substrate side. The free end of the current sensor drains to ground. While both schemes work well for process monitoring, we will use the substrate-side configuration for the experimental results presented below.

The frequency of jetting can be determined by measuring the time elapsed between two successive jets. Each peak in the current signal corresponds to a single jet. This is illustrated in figure 11. For the resolution range (<5 μm) in which we operate, the typical measured current associated with each droplet is found to be in the range of 10 to 100 nA. Thus, the jet current detection capability, while not necessary for pulsed mode E-jetting, is useful for determining the number of droplets released per pulse. This information can then be used for establishing voltage pulse modulation parameters described in sections 3 and 4.

7.2. Printing results

We demonstrate additional capabilities of the high-speed pulsed E-jet printing regime through the following. Figure 12 shows a time plot of current measurement on the substrate side superimposed on a time plot of the voltage pulse. The ink used was a 10 mM aqueous phosphate buffer solution with 10% (by vol.) glycerol. We observe that a single droplet is released from the micro capillary within the pulse time. This capability directly translates into a drop-on-demand regime for E-jet, which will substantially enhance the applicability of E-jet for printing bio-sensors, among other applications.

Figure 13 shows the measured current plot for a train of voltage pulses and the corresponding droplet ejections. We note that multiple droplets (in this case, four) are ejected within each pulse period. By changing the pulse time (T_p), the number of droplets ejected per pulse can be controlled.

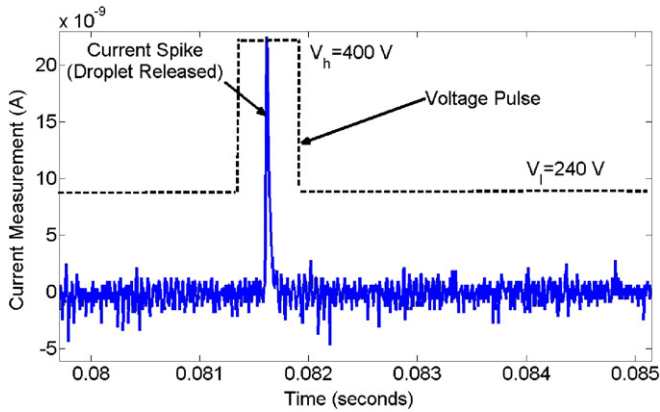


Figure 12. Plot of current measurement showing a voltage pulse and the corresponding peak of a single droplet.

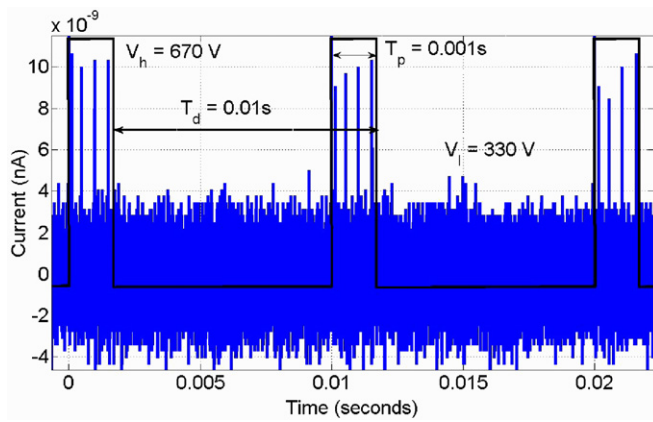


Figure 13. Plot of current measurement showing a voltage pulse train with multiple droplets released per pulse.

Through varying pulse time, multiple droplets can jet within the pulse width and coalesce to create different droplet sizes. Figure 14 shows a plot of varying pulse width (T_p) against droplet diameter (D) on the substrate. The ink was a UV curable polyurethane ink; jetting was accomplished

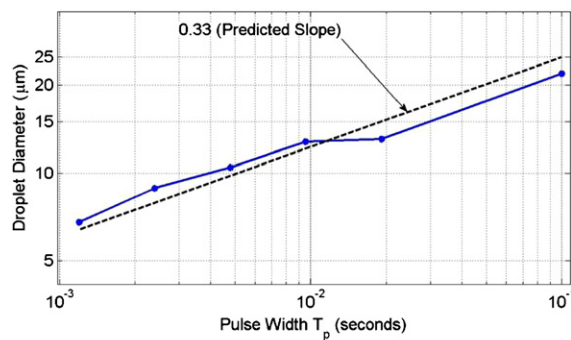


Figure 14. Plot of droplet diameter on the surface (D) against the pulse width T_p . The predicted slope of 0.33 is plotted as a dashed line. We see good correlation between the prediction and the measurement values.

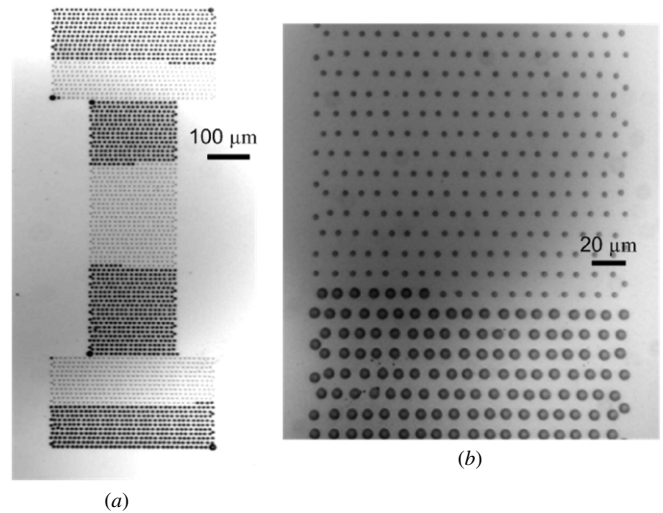
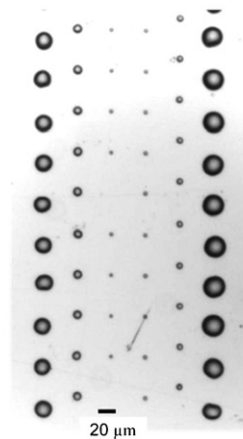


Figure 15. (a) Printed pattern using NOA 73 from a 5 μm micro capillary, with on-the-fly droplet diameter control by changing the pulse width T_p . (b) Detail of pattern showing controlled transition from 3.9 to 8.1 μm droplet size. The droplet size is controlled independent of droplet spacing (16 μm).

through using a micro capillary nozzle of inner diameter (ID) 5 μm . The droplet diameter varied from 6 to 22 μm based on the duration of the pulse width.

The pulsed mode operation of the E-jet process enables on-the-fly droplet diameter change. This is illustrated in figure 15. The droplet diameter is varied by changing the pulse width and generates denser and less dense printed areas without the need for changing nozzle tips, readjustment of voltage or change in deposition frequency. We therefore independently control droplet diameter and droplet spacing, as mentioned in section 3.

This independent control of droplet spacing and droplet diameter can be exploited to create patterns with varying density of droplets or varying droplet size that can be adjusted on the fly. Figure 15 demonstrates this capability in a printed pattern using NOA 73 from a 5 μm micro capillary. The



droplet size is varied by changing the pulse width (T_p) from 500 to 2500 μs . The resulting average droplet size is found to be 3.9 μm and 8.1 μm respectively for the two cases, with standard deviations of 0.4 μm and 0.3 μm (with 16 random droplet diameter measurements). The droplet spacing (16 μm) is unaffected by changes in droplet size.

8. Conclusions

E-jet printing technology has shown tremendous potential for applications in printed electronics, biotechnology and micro-electromechanical devices. Printing speed and droplet size control present the biggest challenge for jet-printing techniques. In order to address these issues simultaneously, a high-speed high-precision E-jet printing technique was investigated. By using a pulsed dc voltage signal to produce E-jetting, precise droplet placement and droplet spacing was obtained at very fast printing speeds. The printing times were cut down by three orders of magnitude, while delivering specified droplet deposition rates and feature sizes. Further, the proposed method also demonstrated drop-on-demand capability, as well as on-the-fly droplet feature size and droplet volume control.

Acknowledgments

The authors gratefully acknowledge the contribution and support of the NSF Nano-CEMMS Center under award number DMI-0328162 and CMMI-0749028.

References

- [1] Park J-U et al 2007 *Nature Mater.* **6** 782–9
- [2] Lee D-Y, Lee J C, Shin Y-S, Park S-E, Yu T-U, Kim Y-J and Hwang J 2008 *J. Phys.: Conf. Ser.* **142** 012039
- [3] Park J-U, Lee S, Unarunotai S, Sun Y, Dunham S, Song T, Ferreira P M, Alleyne A G, Paik U and Rogers J A 2010 *Nano Lett.* **2** 584–91
- [4] Park J-U, Lee J H, Paik U, Lu Y and Rogers J A 2008 *Nano Lett.* **8** 4210–6
- [5] <http://technologyreview.com/computing/19373/page1/>
- [6] Jaworek A and Krupa A 1996 *J. Aerosol Sci.* **27** 979–86
- [7] Juraschek R and Rollgen F W 1998 *Int. J. Mass Spectrom.* **177** 1–15
- [8] Choi H K, Park J-U, Park O O, Ferreira P M, Georgiadis J G and Rogers J A 2008 *Appl. Phys. Lett.* **92** 123109
- [9] Chen C H, Saville D A and Aksay I A 2006 *Appl. Phys. Lett.* **89** 124103(1)–(3)
- [10] Kim Y-J, Kim S-Y, Lee J-S, Hwang J and Kim Y-J 2009 *J. Micromech. Microeng.* **19** 107001
- [11] Nguyen V D and Byun D 2009 *Appl. Phys. Lett.* **94** 173509
- [12] Kim J, Oh H and Kim S-S 2008 *J. Aerosol Sci.* **39** 819–25
- [13] Stachewicz U, Yurteri C U, Marijnissen J C M and Dijkman J F 2009 *Appl. Phys. Lett.* **95** 224105
- [14] Stachewicz U, Dijkman J F, Burdinski D, Yurteri C U and Marijnissen J C M 2009 *Langmuir* **25** 2540–9
- [15] Cloupeau M and Prunet-Foch B 1994 *J. Aerosol Sci.* **25** 1021–36
- [16] Taylor G 1969 *Proc. R. Soc. Lond. A.* **313** 453–75